MATCH
Communications in Mathematical and in Computer Chemistry

MATCH Commun. Math. Comput. Chem. **75** (2016) 629-652

ISSN 0340 - 6253

Simulation Study of Nonlinear Reverse Osmosis Desalination System Using Third and Fourth Chebyshev Wavelet Methods

Ali Merina Houria[a], Belhamiti Omar[a]

[a] *Laboratory of Pure and Applied Mathematics, Abdelhamid Ibn Badis University, Mostaganem 27000, Algeria*

alimerinaho@yahoo.fr, belhamitio@yahoo.fr

(Received August 3, 2015)

Abstract

This paper is concerned with introducing four wavelets collocation algorithms combined with decoupling and quasi-linearization technique for solving a small-scale reverse osmosis desalination problem represented by a system of four strongly nonlinear coupled differential equations. The basic idea for obtaining numerical solutions for such system is to combine every one of the four kinds Chebyshev wavelets with the decoupling and quasi-linearization technique to transform each differential equation to a linear algebraic system which can be efficiently solved. The model is verified using the experimental data existing in the literature. In addition, an illustrative example is presented to demonstrate the convergence, efficiency and accuracy of the proposed method.

1 Introduction

Wavelet theory is a recent mathematical topic that has a great variety of possible applications. Wavelets, as a concept, is related to several disciplines (engineering, physics and pure mathematics). The present success of the wavelets is mainly due to the growing interest of mathematics and other sciences in their applications. The wavelets have many applications in different domain. In fact, they have led to stimulate applications in signal analysis [15, 20, 21]. Other applications in numerical analysis can be found in [11, 28]. Moreover, the operational matrices of integration for the Haar, Chebyshev and Legendre wavelets have been developed in [17,28,38]. In the literature, there is a great concentration on the first and the second kinds of Chebyshev wavelets and their various uses in numerous applications. For instance, the authors in [7] found numerical solutions of differential equations and multi-order fractional differential equations by using the first kind of Chebyshev wavelets. Then, in [12, 18], the authors employed a Chebyshev wavelets approach for nonlinear systems of Volterra integral equations as well as for singular boundary value problems. For more details on solving partial and fractional differential equations using the second kind of Chebyshev wavelet method, we refer the reader to [24, 35]. In a recent contribution [5], W.M. Abd-Elhameed used a spectral second kind Chebyshev wavelets algorithm to solve second-order differential equations of Bratu type. More recently, [39], L. Zhu and Y. Wang developed a second kind of Chebyshev wavelet operational matrix of integration with some applications in the calculus of variations.

In order to use the Chebyshev wavelets for solving nonlinear differential systems, the decoupling and quasi-linearization technique (DQLT) is introduced in this paper. The DQLT has been presented in the first time by Bellman and Kalaba as a generalization of the Newton–Raphson method [10]. The main advantage of Bellmann-Kalaba method, in addition to quadratic convergence, is that it allows to decouple and linearize strongly nonlinear differential equations. We refer the reader to [9, 33] for some applications on ordinary differential equations and [26, 34] for other applications on reaction diffusion problems.

Let us now introduce the seawater desalination process which is the focus of our work. This process has been considered as one of the most promising techniques for supplying fresh water in the regions suffering from water scarcity. Two technologies are used around the world for desalination: thermal or membrane. This later is implemented through two main processes: reverse osmosis (RO) and electrodialysis (ED). The reverse osmosis desalination system (RODS) has appeared to be a powerful process; it is based on overcoming the natural phenomena of osmotic pressure, which occurs when a semi-permeable membrane separates two solutions with different concentrations of ions. Many mathematical models have been developed to describe the behaviour of the RODS. For more details, we cite [1, 2, 22, 25].

The main purpose of this work is to present a new approach based on the four kinds of Chebychev polynomials. We give more importance to the third and fourth kinds, since, the first and the second kinds were sufficiently studied. As an application to show the efficiency of the proposed approach, we are interested by the model developed for the hollow-fiber membrane modules with co-corrent flow, described in [3]. The reverse osmosis desalination system (RODS) is represented by a set of strongly nonlinear coupled differential equations which are solved. The obtained results are reliable and very close to the reality [32, 36]. The numerical resolution of the mathematical model is carried out using a new approach which consists, firstly, applies the iterative DQLT to separate and linearize the system. Then, at each iteration, we use the Chebyshev wavelets methods to solve the resulting equations.

The remainder of the paper is organized as follows : In Section 2, we introduce the RO desalination system. Section 3 presents the main steps that we need in the Chebyshev wavelets methods. To clarify the approach, Section 4 is devoted to simulate the reverse osmosis problem. At the end, a conclusion follows.

2 Modeling of Reverse Osmosis Desalination System

Seawater desalination is a feasible option for potable water production, since available water sources are gradually depleting due to water scarcity as well as quality deterioration [37] [6]. Among all the available desalination approaches, reverse osmosis is the most promising and widely applied technology for water desalination due to its low capital cost, high energy efficiency, and its simplicity in operation [8, 13, 14, 16, 27]. Reverse osmosis (RO) is a water purification technology that uses a semipermeable membrane to remove larger particles from drinking water. The osmotic pressure created by the concentration gradient drives the flow of water from the dilute solution to the concentrated solution, until chemical equilibrium is established. The flow of water can be reversed with the application of an external hydraulic force (pressure) if this force is greater than the osmotic pressure. RO membranes are designed to retain salts and low-molecular weight solutes while allowing water to pass through. Membranes are implemented in several types of modules. There are two main types, called the tubular membrane system and plate & frame membrane system. Tubular modules are constituted of two concentric tubes designed to separate a given feed into a higher pressure stream (retentate) and alow pressure stream (permeate) see figure 2. According to the flow circulation inside the membrane, two types of flow can be distinguished: the co-current and counter-current

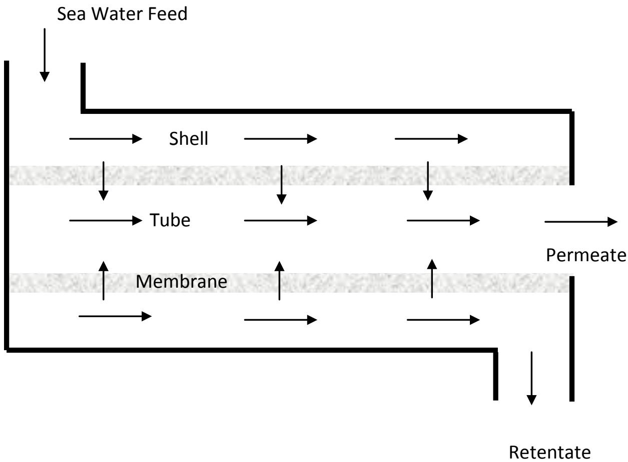

Figure 1: Hollow fiber membrane.

flow patterns

A mathematical model is used to control better the performance of hollow fiber reverse osmosis membrane with co-corrent flow. The model is based on the solution-diffusion mass transfer model and takes into account the effect of the flow pattern of the permeate in the membrane.

In this paper, the model chosen to describe the salt and water fluxes across the membrane is that developed by the author [3]. It consists of a set of four strongly nonlinear differential equations. This system is found according to material balance principle and Fick's law which is:

$$\begin{cases} \dfrac{dQ_{sw}}{dx} = -\pi \dfrac{A_w}{\sigma_w} D_m \left(\Delta P - \kappa \left(\dfrac{\dot{Q}_{ss}}{Q_{sw}} - \dfrac{\dot{Q}_{fs}}{Q_{fw}} \right) \right) \\ \dfrac{dQ_{fw}}{dx} = \pi \dfrac{A_w}{\sigma_w} D_m \left(\Delta P - \kappa \left(\dfrac{\dot{Q}_{ss}}{Q_{sw}} - \dfrac{\dot{Q}_{fs}}{Q_{fw}} \right) \right) \\ \dfrac{d\dot{Q}_{ss}}{dx} = -\pi B_s D_m \left(\dfrac{\dot{Q}_{ss}}{Q_{sw}} - \dfrac{\dot{Q}_{fs}}{Q_{fw}} \right) \\ \dfrac{d\dot{Q}_{fs}}{dx} = \pi B_s D_m \left(\dfrac{\dot{Q}_{ss}}{Q_{sw}} - \dfrac{\dot{Q}_{fs}}{Q_{fw}} \right), \end{cases} \tag{1}$$

where

Q_{sw} is the water volumetric flow rate in the shell side,

Q_{fw} is the water volumetric flow rate in the fiber side,

$\dot{Q}_{ss}$ represents the solute mass flow rate in the shell side,

$\dot{Q}_{fs}$ the solute mass flow rate in the fiber side,

κ is a proportionality coefficient,

A_w is the water permeability coefficient (a function of the salt diffusivity through the membrane),

ΔP is the applied pressure driving force (a function of the feed, concentrate and permeate concentrations),

σ_w is the water density,

B_s is the solute permeability coefficient,

The osmotic pressure is approximately represented by a linear function of solute concentrations

$$\pi = \kappa C.$$

3 Some Preliminaries

3.1 Chebyshev polynomials and their properties

In this subsection, we are interested in the main properties of the four kinds of Chebyshev polynomials, which are particular cases of the Jacobi ones. Jacobi polynomials, denoted by $J_m^{(\alpha,\beta)}(x)$, are generated by the three-term following recursive formula, they are defined over $[-1,1]$, for each $\alpha, \beta > -1$

$$\begin{cases} J_0^{(\alpha,\beta)}(x) = 1, \\ J_1^{(\alpha,\beta)}(x) = (\alpha+1) + (\alpha+\beta+2)\left(\frac{x-1}{2}\right), \\ a_{m,0} J_m^{(\alpha,\beta)}(x) = (a_{m,1}x - a_{m,2})\, J_{m-1}^{(\alpha,\beta)}(x) - a_{m,3} J_{m-2}^{(\alpha,\beta)}(x), \end{cases}$$

where,

$$\begin{cases} a_{m,0} = 2m(\alpha+\beta+m)(\alpha+\beta+2m-2), \\ a_{m,1} = (\alpha+\beta+2m-1)(\alpha+\beta+2m-2)(\alpha+\beta+2m), \\ a_{m,2} = (\alpha^2+\beta^2)(\alpha+\beta+2m-1), \\ a_{m,3} = 2(\alpha+m-1)(\beta+m-1)(\alpha+\beta+2m). \end{cases}$$

The family $\left\{J_n^{(\alpha,\beta)}(x)\right\}_{n\in\mathbb{N}}$ forms a basis for the space $L^2_{\omega^{(\alpha,\beta)}}(-1,1)$ with the weighted function $\omega^{(\alpha,\beta)}(x) = (1-x)^\alpha(1+x)^\beta$ [19].

The table gives the four kinds of Chebyshev polynomials (see [23], [29])

An important property of the Chebyshev polynomials is the orthogonality with respect to the weighted function $\omega^{(k)}(x)$ with its k^{th} kind, $k = 1, .., 4$ i.e.:

$$\left\langle T_n^{(k)}, T_m^{(k)} \right\rangle_{\omega^{(k)}} = \int_{-1}^{1} T_n^{(k)}(x)\, T_m^{(k)}(x)\, \omega^{(k)}(x)\, dx = \lambda_n^{(k)} \delta_{n,m},$$

Table 1: The four kinds of Chebyshev polynomials.

Types of Chebyshev polynomials	The recursive formula	The weight function
The first kind	$T_1^{(1)}(x)=1,T_1^{(1)}(x)=x,$ $T_m^{(1)}(x)=2xT_{m-1}^{(1)}-T_{m-2}^{(1)},$	$\omega^{(1)}(x)=(1-x)^{-1/2}(1+x)^{-1/2}$
The second kind	$T_1^{(2)}(x)=1,T_1^{(2)}(x)=2x,$ $T_m^{(2)}(x)=2xT_{m-1}^{(2)}-T_{m-2}^{(2)},$	$\omega^{(2)}(x)=(1-x)^{1/2}(1+x)^{1/2}$
The third kind	$T_1^{(3)}(x)=1,T_1^{(3)}(x)=2x-1,$ $T_m^{(3)}(x)=2xT_{m-1}^{(3)}-T_{m-2}^{(3)},$	$\omega^{(3)}(x)=(1-x)^{-1/2}(1+x)^{1/2}$
The fourth kind	$T_1^{(4)}(x)=1,T_1^{(4)}(x)=2x+1,$ $T_m^{(4)}(x)=2xT_{m-1}^{(4)}-T_{m-2}^{(4)},$	$\omega^{(4)}(x)=(1-x)^{1/2}(1+x)^{-1/2}$

where $\langle .,. \rangle_{\omega^{(k)}}$ denotes the inner product in the weighted space $L^2_{\omega^{(k)}}(-1,1)$, $\delta_{n,m}$ is the Kronecker function and $\lambda_n^{(k)}=\left\|T_n^{(k)}\right\|^2_{\omega^{(k)}}$ is defined as:

$$\lambda_n^{(1)}=\begin{cases}\pi, \text{if } n=0\\ \dfrac{\pi}{2}, \text{if } n\neq 0\end{cases}$$

and

$$\lambda_n^{(k)}=\begin{cases}\dfrac{\pi}{2}, \text{if } k=2\\ \pi, \text{if } k=3,4.\end{cases}$$

3.2 Chebyshev Wavelets

We define the four kinds of Chebyshev wavelets on the interval $[0,1]$ as follows:

$$\psi_{n,m}^{(k)}(x)=\begin{cases}\frac{1}{\sqrt{\lambda^{(k)}}}2^{\frac{j}{2}}\widetilde{T_m}^{(k)}\left(2^jx-2n+1\right), & \frac{n-1}{2^{j-1}}\leqslant x<\frac{n}{2^{j-1}}\\ 0, \text{otherwise}\end{cases} \tag{2}$$

where,

$$\frac{1}{\sqrt{\lambda^{(1)}}}\widetilde{T_m}^{(1)}(x)=\begin{cases}\frac{1}{\sqrt{\pi}}, m=0\\ \sqrt{\frac{2}{\pi}}T_m^{(1)}(x), m>0,\end{cases}$$

and

$$\frac{1}{\sqrt{\lambda^{(k)}}}\widetilde{T_m}^{(k)}(x)=\begin{cases}\sqrt{\frac{2}{\pi}}T_m^{(2)}(x), \text{if } k=2\\ \frac{1}{\sqrt{\pi}}T_m^{(3)}(x), \text{if } k=3\\ \frac{1}{\sqrt{\pi}}T_m^{(4)}(x), \text{if } k=4.\end{cases}$$

The integer $m=0,1,...,M-1$ denotes the order of Chebyshev polynomials, ($M\in\mathbb{N}^*$ represents the number of collocation points on each level) and $n=1,2,...,2^{j-1}$ denotes the number of decomposition levels (with $j\in\mathbb{N}^*$), $T_m^{(k)}(x)$ is the k^{th} kind of chebyshev polynomial.

Remark 1 *For a fixed $n \in \{1, 2, \ldots, 2^{j-1}\}$, the family*

$$\left\{\lambda_j^{(k)} \overline{T}_m^{(k)}(x)\right\}_{m\in\mathbb{N}}, \qquad \textit{for each } k = \overline{1,4}$$

forms an orthonormal basis of the weighted space

$$L^2_{\omega_n^{(k)}}\left(\left[\frac{n-1}{2^{j-1}}, \frac{n}{2^{j-1}}\right]\right),$$

where $\omega_n^{(k)}(x) = \omega^{(k)}(2^j x - 2n + 1)$, $\overline{T}_m^{(k)}(x) = T_m^{(k)}(2^j x - 2n + 1)$ and

$$\lambda_j^{(k)} = 2^{j/2}\begin{cases} \sqrt{\frac{2}{\pi}}, & \textit{if } k = 1, 2 \\ \frac{1}{\sqrt{\pi}}, & \textit{if } k = 3, 4 \end{cases}$$

represents the normalization coefficient.

For example, the family of the third kind Chebyshev wavelet can be expressed on the n^{th} level by

$$\begin{cases} \psi_{n,0}^{(3)}(x) = \dfrac{2^{\frac{j}{2}}}{\sqrt{\pi}}, \\ \psi_{n,1}^{(3)}(x) = \dfrac{2^{\frac{j}{2}}}{\sqrt{\pi}}\left(2^{j+1}x - 4n + 1\right), \\ \psi_{n,2}^{(3)}(x) = \dfrac{2^{\frac{j}{2}}}{\sqrt{\pi}}\left(2^{2(j+1)}x^2 - 2^{j+1}(8n-3)x + (16n^2 - 12n + 1)\right), \\ \vdots \\ \psi_{n,M-1}^{(3)}(x) = \dfrac{2^{\frac{j}{2}}}{\sqrt{\pi}} T_{M-1}^{(3)}\left(2^j x - 2n + 1\right). \end{cases}$$

For $j = 2$ and $M = 3$, we have

$$\begin{cases} \psi_{1,0}^{(3)}(x) = \frac{2}{\sqrt{\pi}} \\ \psi_{1,1}^{(3)}(x) = \frac{2}{\sqrt{\pi}}(8x - 3) \\ \psi_{1,2}^{(3)}(x) = \frac{2}{\sqrt{\pi}}(64x^2 - 40x + 5) \end{cases} \qquad 0 \leqslant x < \frac{1}{2}$$

$$\begin{cases} \psi_{2,0}^{(3)}(x) = \frac{2}{\sqrt{\pi}} \\ \psi_{2,1}^{(3)}(x) = \frac{2}{\sqrt{\pi}}(8x - 7) \\ \psi_{2,2}^{(3)}(x) = \frac{2}{\sqrt{\pi}}(64x^2 - 104x + 41) \end{cases} \qquad \frac{1}{2} \leqslant x < 1.$$

3.3 Approximation Functions

We assume that

$$f_n \in L^2_{\omega_n^{(k)}}\left(\left[\frac{n-1}{2^{j-1}}, \frac{n}{2^{j-1}}\right[\right),$$

where f_n represents the restriction of f on the interval $\left[\frac{n-1}{2^{j-1}}, \frac{n}{2^{j-1}}\right[$. It can be expanded as

$$f_n(x) = \sum_{m=0}^{+\infty} c_{n,m} \overline{T}_m^{(k)}(x), \tag{3}$$

where

$$c_{n,m} = \left\langle f_n, \lambda_j^{(k)} \overline{T}_m^{(k)} \right\rangle_{\omega_n^{(k)}}$$

and

$$\overline{T}_m^{(k)}(x) = T_m^{(k)}\left(2^j x - 2n + 1\right).$$

We have

$$f(x) = \sum_{n=1}^{2^{j-1}} f_n(x) = \sum_{n=1}^{2^{j-1}} \sum_{m=0}^{+\infty} c_{n,m} \psi_{n,m}^{(k)}(x). \tag{4}$$

On the other hand, the series (3) is truncated as

$$f_n(x) \approx \sum_{m=0}^{M-1} c_{n,m} \overline{T}_m^{(k)}(x),$$

and then, for all x into $[0,1]$, we can write

$$f(x) = \sum_{n=1}^{2^{j-1}} f_n(x) \approx \sum_{n=1}^{2^{j-1}} \sum_{m=0}^{M-1} c_{n,m} \psi_{n,m}^{(k)}(x) = C^T \Psi^{(k)}(x), \tag{5}$$

where C and $\Psi^{(k)}(x)$ are $2^{j-1}M$ vectors given by:

$$\begin{aligned} C &= \left[c_{1,0}, \ldots, c_{1,M-1}, c_{2,0}, \ldots, c_{2,M-1}, \ldots\ldots, c_{2^{j-1},0}, \ldots, c_{2^{j-1},M-1}\right]^T, \qquad (6)\\ \Psi^{(k)}(x) &= \left[\psi_{1,0}^{(k)}(x), \ldots, \psi_{1,M-1}^{(k)}(x), \ldots, \psi_{2^{j-1},0}^{(k)}(x), \ldots, \psi_{2^{j-1},M-1}^{(k)}(x)\right]^T. \end{aligned}$$

3.4 Convergence results

Theorem 2 *Let f be a second-order derivative square-integrable function defined on* $[0,1]$ *whose second-order derivative is bounded by a positive constant K.*

We have

1. *For $m > 1$ and $1 \leqslant n \leqslant 2^{j-1}$, the following inequalities are valid:*

$$\left|c_{nm}^{(k)}\right| \leqslant \begin{cases} \frac{2^{-\frac{j}{2}}}{4} \frac{K}{m(m-1)}, & \text{if } k = 1 \\ \frac{2^{-\frac{5j}{2}}}{4} \frac{K}{m(m-1)}, & \text{if } k = 2, 3, 4. \end{cases}$$

2. *The infinite series given in (4) converges uniformly on* $[0,1]$.

Proof.

1. Substituting the expression of $\psi_{nm}^{(3)}(x)$ in $c_{n,m}^{(3)}$, we have

$$c_{n,m}^{(3)} = \frac{2^{\frac{j}{2}}}{\sqrt{\pi}} \int_{\frac{n-1}{2^{j-1}}}^{\frac{n}{2^{j-1}}} u\left(x\right) T_m^{(3)}\left(2^j x - 2n + 1\right) \omega_n^{(3)}\left(x\right) dx.$$

Let $t = 2^j x - 2n + 1$, it yields then that

$$c_{n,m}^{(3)} = \frac{2^{\frac{-j}{2}}}{\sqrt{\pi}} \int_{-1}^{1} u\left(\frac{t + 2n - 1}{2^j}\right) T_m^{(3)}\left(t\right) \sqrt{\frac{(1+t)}{(1-t)}} dt.$$

By taking $t = \cos\theta$ and using the trigonometric forms of the third kind Chebyshev polynomials (see [23]), it follows

$$\begin{aligned} c_{n,m} &= \frac{2^{\frac{-j}{2}}}{\sqrt{\pi}} \int_0^{\pi} f_n\left(\frac{\cos\left(\theta\right) + 2n - 1}{2^j}\right) \frac{\cos\left(\left(m + \frac{1}{2}\right)\theta\right)}{\cos\left(\frac{\theta}{2}\right)} \left(1 + \cos\theta\right) d\theta \\ &= \frac{2^{\frac{-j}{2}}}{\sqrt{\pi}} \int_0^{\pi} f_n\left(\frac{\cos\left(\theta\right) + 2n - 1}{2^j}\right) \left[\cos\left(\left(m+1\right)\theta\right) + \cos\left(m\theta\right)\right] d\theta. \end{aligned}$$

Using an integration by parts twice, we have

$$\begin{aligned} c_{n,m} = \; & \frac{1}{4}\frac{2^{\frac{-5j}{2}}}{\sqrt{\pi}} \int_0^{\pi} f_n''\left(\frac{\cos\left(\theta\right) + 2n - 1}{2^j}\right) \left(\frac{\left(\cos((m-1)\,\theta) - \cos((m+1)\,\theta)\right)}{m\left(m+1\right)}\right. \\ & - \frac{\left(\cos((m+1)\,\theta) - \cos((m+3)\,\theta)\right)}{\left(m+1\right)\left(m+2\right)} + \frac{\left(\cos((m-2)\,\theta) - \cos(m\theta)\right)}{m\left(m-1\right)} \\ & \left. - \frac{\left(\cos(m\theta) - \cos((m+2)\,\theta)\right)}{m\left(m+1\right)}\right) d\theta \end{aligned}$$

Using the fact that $|f_n''(x)| \leqslant K$ and thanks to Cauchy-Schwarz inequality, it follows

$$\begin{aligned} \left|c_{n,m}\right|^2 \leqslant \; & \frac{2^{-5j}}{16\pi} K^2 \left(\int_0^{\pi} \left|\frac{\left(\cos((m-1)\,\theta) - \cos((m+1)\,\theta)\right)}{m\left(m+1\right)}\right|^2 d\theta\right. \\ & + \int_0^{\pi} \left|\frac{\left(\cos((m+1)\,\theta) - \cos((m+3)\,\theta)\right)}{\left(m+1\right)\left(m+2\right)}\right|^2 d\theta \\ & + \int_0^{\pi} \left|\frac{\left(\cos((m-2)\,\theta) - \cos(m\theta)\right)}{m\left(m-1\right)}\right|^2 d\theta \\ & \left. + \int_0^{\pi} \left|\frac{\left(\cos(m\theta) - \cos((m+2)\,\theta)\right)}{m\left(m+1\right)}\right|^2 d\theta\right) \\ \leqslant \; & \frac{2^{-5j}}{16\pi} K^2 \left(\frac{\pi}{m^2\left(m+1\right)^2} + \frac{\pi}{\left(m+1\right)^2\left(m+2\right)^2}\right. \\ + \; & \left. \frac{\pi}{m^2\left(m-1\right)^2} + \frac{\pi}{m^2\left(m+1\right)^2}\right) \leqslant \frac{2^{-5j}}{16} \frac{K^2}{m^2\left(m-1\right)^2} \end{aligned}$$

2. Since, (see [30])

$$\left|\psi_{nm}^{(3)}\left(x\right)\right| \leqslant 2^{\frac{j}{2}} \sqrt{\frac{m}{\pi}},$$

then, we have

$$\left|c_{n,m}\psi_{nm}^{(3)}(x)\right| \leqslant \frac{2^{-2j}K}{4\sqrt{\pi}}\frac{1}{\sqrt{m}(m-1)}$$

and

$$E_{j,M}^{(k)}(x) = \sum_{n=1}^{2^{j-1}}\sum_{m=0}^{\infty} c_{n,m}\psi_{n,m}^{(k)}(x) - \sum_{n=1}^{2^{j-1}}\sum_{m=0}^{M-1} c_{n,m}\psi_{n,m}^{(k)}(x) = \sum_{n=1}^{2^{j-1}}\left(\sum_{m=M}^{\infty} c_{n,m}\psi_{n,m}^{(k)}(x)\right)$$

$$\left|E_{j,M}^{(3)}(x)\right| \leqslant \sum_{n=1}^{2^{j-1}}\sum_{m=M}^{\infty}\left|c_{n,m}\psi_{n,m}^{(3)}(x)\right| \leqslant \frac{2^{-2j}K}{4\sqrt{\pi}}\sum_{n=1}^{2^{j-1}}\sum_{m=M}^{\infty}\frac{1}{\sqrt{m}(m-1)}.$$

We conclude that this last series is convergent.

In the same manner, we obtain

$$\left|E_{j,M}^{(1)}(x)\right| \leqslant \frac{2^{-2j}K}{4}\sqrt{\frac{2}{\pi}}\sum_{n=1}^{2^{j-1}}\sum_{m=M}^{\infty}\frac{1}{m(m-1)},$$

$$\left|E_{j,M}^{(2)}(x)\right| \leqslant \frac{2^{-2j}K}{4}\sqrt{\frac{2}{\pi}}\sum_{n=1}^{2^{j-1}}\sum_{m=M}^{\infty}\frac{1}{\sqrt{m}(m-1)}$$

and

$$\left|E_{j,M}^{(4)}(x)\right| \leqslant \frac{2^{-2j}K}{4\sqrt{\pi}}\sum_{n=1}^{2^{j-1}}\sum_{m=M}^{\infty}\frac{1}{\sqrt{m}(m-1)}.$$

■

3.5 Operational Matrix of Integration and Wavelets Product

In this subsection, we introduce the operational matrices of integration for each wavelet described above.

Theorem 3 *The integration of the k^{th} kind Chebyshev wavelets $\Psi^{(k)}(t)$, defined in (2), can be approximated as follows:*

$$\int_0^t \Psi^{(k)}(\tau)\,d\tau \approx P^{(k)}\Psi^{(k)}(t), \tag{7}$$

where $P^{(k)}$ denotes the $2^{j-1}M \times 2^{j-1}M$ operational matrix of integration given by

$$P^{(k)} = \begin{bmatrix} L^{(k)} & F^{(k)} & \cdots & F^{(k)} \\ 0 & L^{(k)} & \ddots & \vdots \\ \vdots & \ddots & \ddots & F^{(k)} \\ 0 & \cdots & 0 & L^{(k)} \end{bmatrix},$$

$For\ k=1,$

$$L^{(1)}_{p,q}=2^{-j}\times\begin{cases}1 \quad for\ p=1\ \ and\ q=1\\ -\dfrac{\sqrt{2}}{4} \quad for\ p=2\ \ and\ q=1\\ \dfrac{\sqrt{2}}{2} \quad for\ p=1\ \ and\ q=2\\ \dfrac{1}{2p} \quad for\ p=2,...,M-1\ \ and\ q=p+1\\ \dfrac{-1}{(2(p-2)+2)} \quad for\ p=3,...,M\ \ and\ q=p-1\\ \dfrac{(-1)^p\sqrt{2}}{p(p-2)} \quad for\ \ p=3,...,M\ \ and\ q=1\\ 0 \qquad otherwise\end{cases}$$

$$F^{(1)}_{p,q}=2^{-j}\times\begin{cases}2 \quad q=p=1\\ 0 \quad p=2,q=1\\ \dfrac{-2mod(p,2)}{p\,(p-2)} \quad for\ \ q=1\ \ and\ p=3,...,M\\ 0 \qquad otherwise\end{cases}$$

$For\ k=2,$

$$L^{(2)}_{p,q}=2^{-j}\times\begin{cases}1 \quad for\ p=1\ \ and\ q=1\\ -\frac{3}{4} \quad for\ p=2\ \ and\ q=1\\ \dfrac{1}{2p} \quad for\ p=2,...,M-1\ \ and\ q=p+1\\ \dfrac{-1}{2(p+1)} \quad for\ p=3,...,M\ \ and\ q=p-1\\ \dfrac{(-1)^{p+1}}{p} \quad for\ \ p=3,...,M\ \ and\ q=1\\ 0 \qquad otherwise\end{cases}$$

$$F^{(2)}_{p,q}=2^{-j}\times\begin{cases}\dfrac{2mod(p+2,2)}{p} \quad for\ \ q=1\ \ and\ p=1,...,M\\ 0 \qquad otherwise\end{cases}$$

$For\ k=3,$

$$L^{(3)}_{p,q}=2^{-j}\times\begin{cases}\dfrac{3}{2} \quad for\ p=1\ \ and\ q=1\\ -2 \quad for\ p=2\ \ and\ q=1\\ \dfrac{-1}{(2p(p-1))}..for\ p=q=2,...,M\\ \dfrac{-1}{2p} \quad for\ p=2,...,M-1\ \ and\ q=p+1\\ \dfrac{-1}{2(p-1)} \quad for\ p=3,...,M\ \ and\ q=p-1\\ \dfrac{(-1)^{p+1}(2p-1)}{p(p-1)} \quad for\ \ p=3,...,M\ \ and\ q=1\\ 0 \qquad otherwise\end{cases}$$

$$F^{(3)}_{p,q}=2^{-j}\times\begin{cases}\dfrac{(-1)^{(p+1)}2}{(p-mod\,(p+1,2))} \quad if\ \ q=1\ \ and\ p\geqslant 2\\ 0 \qquad otherwise\end{cases}$$

For $k=4$,

$$L_{p,q}^{(4)} = 2^{-j} \times \begin{cases} \frac{1}{2} \quad for\ p=1\ \ and\ q=1 \\ 0 \quad for\ p=2\ \ and\ q=1 \\ \dfrac{1}{(2p(p-1))} ..for\ p=q=2,...,M \\ \dfrac{1}{2p} \quad for\ p=2,...,M-1\ \ and\ q=p+1 \\ \dfrac{-1}{2p} \quad for\ p=3,...,M-1\ \ and\ q=p-1 \\ \dfrac{(-1)^p}{p(p-1)} \quad for\ \ p=3,...,M\ \ and\ q=1 \\ 0 \qquad otherwise \end{cases}$$

$$F_{p,q}^{(4)} = 2^{-j} \times \begin{cases} \dfrac{2}{p-mod(p+1,2)} \quad if\ \ q=1\ \ and\ for\ all\ p \\ 0 \qquad otherwise \end{cases}$$

where, $mod(.,.)$ *represents the division remainder between two given numbers.*

Lemma 4 *For* $t \in [-1,1]$, *we have*

$$T_{m'}^{(3)}(t) = \frac{1}{2m'(m'+1)2^j}\left[m'\hat{T}_{m'+1}^{(3)\prime}(s) - \hat{T}_{m'}^{(3)\prime}(s) - (m'+1)\hat{T}_{m'-1}^{(3)\prime}(s)\right], \qquad (8)$$

where

$$T_{m'}^{(3)\prime}(t) = \frac{1}{2^j}\hat{T}_{m'}^{(3)\prime}(s)$$

and $t = 2^j s - 2n' + 1$.

For more details, see [4].

Proof. (Theorem 3) It is well known that, for $n' = 1,...,2^{j-1}$and $m' = 0,...,M-1$, we have

$$\begin{aligned} &\int_0^x \psi_{n',m'}^{(3)}(s)ds \qquad (9) \\ =& \begin{cases} \int_{\frac{n'-1}{2^{j-1}}}^{x} \frac{2^{\frac{j}{2}}}{\sqrt{\pi}} T_{m'}^{(3)}(2^j s - 2n' + 1)\, ds & \text{if } \frac{n'-1}{2^{j-1}} \le x \le \frac{n'}{2^{j-1}} \\ \int_{\frac{n'-1}{2^{j-1}}}^{\frac{n'}{2^{j-1}}} \frac{2^{\frac{j}{2}}}{\sqrt{\pi}} T_{m'}^{(3)}(2^j s - 2n' + 1)\, ds & \text{if } x > \frac{n'}{2^{j-1}} \\ 0 \quad \text{if } x < \frac{n'-1}{2^{j-1}} \end{cases} \\ =& \sum_{n=1}^{2^{j-1}} \sum_{m=0}^{M-1} c_{n,m}\psi_{n,m}^{(3)}(x) \end{aligned}$$

We discuss the integral (9) according to the value of n'.

- If $n = n'$, then $\frac{n-1}{2^{j-1}} \leqslant x \leqslant \frac{n}{2^{j-1}}$. In this case, we define

$$g(x) := \int_0^x \psi_{n',m'}^{(3)}(s)ds.$$

It is clear that

$$g\left(x\right)=\int\limits_{0}^{x}\frac{2^{\frac{j}{2}}}{\sqrt{\pi}}T_{m'}^{(3)}\left(2^{j}s-2n'+1\right)ds=\sum_{n=1}^{2^{j-1}}\sum_{m=0}^{M-1}c_{n,m}\psi_{n,m}^{(3)}(x),$$

where,

$$c_{n,m}=\int_{0}^{1}\psi_{n,m}\left(x\right)g\left(x\right)\omega_{n}^{(3)}(x)dx.$$

By lemma 4, we obtain

$$\begin{aligned}c_{n,m} &= \int_{\frac{n-1}{2^{j-1}}}^{\frac{n}{2^{j-1}}}\psi_{n,m}\left(x\right)\left(\int_{\frac{n'-1}{2^{j-1}}}^{x}\frac{2^{\frac{j}{2}}}{\sqrt{\pi}}T_{m'}^{(3)}\left(s\right)ds\right)\omega_{n}^{(3)}(x)dx\\ &= \frac{1}{2m'\left(m'+1\right)2^{j}}\left(\left(m'\delta_{m,m'+1}-\delta_{m,m'}-\left(m'+1\right)\delta_{m,m'-1}\right)\right.\\ &\quad\left.-\left(T_{m'+1}^{(3)}\left(-1\right)m'\delta_{m,0}+T_{m'}^{(3)}\left(-1\right)\delta_{m,0}-\left(m'+1\right)T_{m'-1}^{(3)}\left(-1\right)\delta_{m,0}\right)\right)\end{aligned}$$

- If $n>n'$, then $\frac{n'}{2^{j-1}}\leqslant x$. With the same arguments as before, we get

$$\begin{aligned}c_{n,m} &= \int_{\frac{n-1}{2^{j-1}}}^{\frac{n}{2^{j-1}}}\frac{2^{\frac{j}{2}}}{\sqrt{\pi}}T_{m}^{(3)}\left(2^{j}x-2n+1\right)\left(\int_{\frac{n'-1}{2^{j-1}}}^{\frac{n'}{2^{j-1}}}\frac{2^{\frac{j}{2}}}{\sqrt{\pi}}T_{m'}^{(3)}\left(2^{j}s-2n'+1\right)ds\right)\omega_{n}^{(3)}(x)dx\\ &= \frac{1}{2m'\left(m'+1\right)2^{j}}\left(m'T_{m'+1}^{(3)}\left(1\right)\delta_{0,m}-T_{m'}^{(3)}\left(1\right)\delta_{0,m}-\left(m'+1\right)T_{m'-1}^{(3)}\left(1\right)\delta_{0,m}\right.\\ &\quad\left.-m'T_{m'+1}^{(3)}\left(-1\right)\delta_{0,m}+T_{m'}^{(3)}\left(-1\right)\delta_{0,m}+\left(m'+1\right)T_{m'-1}^{(3)}\left(-1\right)\delta_{0,m}\right).\end{aligned}$$

- If $n<n'$, then $x\leqslant\frac{n'-1}{2^{j-1}}$. In this case, we have

$$c_{n,m}=0.$$

Taking into account the above cases, we can write

$$\begin{aligned}&c_{n,m}\\ &= \frac{2^{-j-1}}{m'\left(m'+1\right)}\begin{cases}\left(m'\delta_{m,m'+1}-\delta_{m,m'}-\left(m'+1\right)\delta_{m,m'-1}\right)-\left(T_{m'+1}^{(3)}\left(-1\right)m'\delta_{m,0}\right.\\ \left.+T_{m'}^{(3)}(-1)\delta_{m,0}-\left(m'+1\right)T_{m'-1}^{(3)}\left(-1\right)\delta_{m,0}\right),\text{if } n=n'\\ m'T_{m'+1}^{(3)}\left(1\right)\delta_{0,m}-T_{m'}^{(3)}\left(1\right)\delta_{0,m}-\left(m'+1\right)T_{m'-1}^{(3)}\left(1\right)\delta_{0,m}\\ -m'T_{m'+1}^{(3)}\left(-1\right)\delta_{0,m}+T_{m'}^{(3)}\left(-1\right)\delta_{0,m}+\left(m'+1\right)T_{m'-1}^{(3)}\left(-1\right)\delta_{0,m},\text{if } n>n'\\ 0,\text{if } n<n'\end{cases}\\ &= \sum_{n=1}^{2^{j-1}}\sum_{m=0}^{M-1}c_{n,m}\psi_{n,m}^{(3)}(x)\\ &= \overbrace{\sum_{m=0}^{M-1}c_{n',m}\psi_{n',m}^{(3)}\left(x\right)}^{S_1}+\overbrace{\sum_{n=n'+1}^{2^{j-1}}\sum_{m=0}^{M-1}c_{n,m}\psi_{n,m}^{(3)}\left(x\right)}^{S_2},\end{aligned}$$

where Γ is the Euler Gamma function and

$$\begin{aligned} T^{(3)}_{m'}(-1) &= \frac{\Gamma(\frac{1}{2})\Gamma(m'+\frac{3}{2})(-1)^{m'}}{\Gamma(m'+\frac{1}{2})\Gamma(\frac{3}{2})} \\ T^{(3)}_{m'}(1) &= \frac{\Gamma(\frac{1}{2})\Gamma(m'+\frac{3}{2})}{\Gamma(m'+\frac{1}{2})\Gamma(\frac{3}{2})(2m'+1)}. \end{aligned}$$

As an example, if $m^{'}=1$, we have

$$\begin{aligned} &\int_0^x \psi^{(3)}_{n',1}(s)ds \\ &= \begin{cases} \int_{\frac{n-1}{2^{j-1}}}^{\frac{n}{2^{j-1}}} \psi_{n,m}(x)\left(\int_{\frac{n'-1}{2^{j-1}}}^{x} \frac{2^{\frac{j}{2}}}{\sqrt{\pi}} T^{(3)}_1\left(2^j s - 2n' + 1\right) ds\right) \omega^{(3)}_n(x)dx & \text{if } \frac{n'-1}{2^{j-1}} \le x \le \frac{n'}{2^{j-1}} \\ \int_{\frac{n-1}{2^{j-1}}}^{\frac{n}{2^{j-1}}} \psi_{n,m}(x)\left(\int_{\frac{n'-1}{2^{j-1}}}^{\frac{n'}{2^{j-1}}} \frac{2^{\frac{j}{2}}}{\sqrt{\pi}} T^{(3)}_1\left(2^j s - 2n' + 1\right) ds\right) \omega^{(3)}_n(x)dx & \text{if } x > \frac{n'}{2^{j-1}} \\ 0 \quad \text{if } x < \frac{n'-1}{2^{j-1}} \end{cases} \\ &= \sum_{n=1}^{2^{j-1}} \sum_{m=0}^{M-1} c_{n,m}\psi^{(3)}_{n,m}(x) \\ &= S_1 + S_2 \end{aligned}$$

$$\begin{aligned} S_1 &= \frac{1}{2^j}\left(-2\right)\psi^{(3)}_{n',0}(x) + \left(\frac{-1}{4}\right)\psi^{(3)}_{n',1}(x) + \left(\frac{1}{4}\right)\psi^{(3)}_{n',2}(x) \\ &= \frac{1}{2^j}(L^{(3)}_{1,0}\psi^{(3)}_{n',0}(x) + L^{(3)}_{1,1}\psi^{(3)}_{n',1}(x) + L^{(3)}_{1,2}\psi^{(3)}_{n',2}(x) \end{aligned}$$

$$\begin{aligned} S_2 &= \frac{1}{2^j}\frac{1}{4}\Big(m'T^{(3)}_{m'+1}(1)\,\delta_{0,m} - T^{(3)}_{m'}(1)\,\delta_{0,m} - (m'+1)\,T^{(3)}_{m'-1}(1)\,\delta_{0,m} \\ &\quad -m'T^{(3)}_{m'+1}(-1)\,\delta_{0,m} + T^{(3)}_{m'}(-1)\,\delta_{0,m} + (m'+1)\,T^{(3)}_{m'-1}(-1)\,\delta_{0,m}\Big)\,\psi^{(3)}_{n,0}(x). \\ &= -2\frac{1}{2^j}\sum_{n=n'+1}^{2^{j-1}} \psi^{(3)}_{n,0}(x) \\ &= F^{(3)}_{1,0}\sum_{n=n'+1}^{2^{j-1}} \psi^{(3)}_{n,0}(x) \end{aligned}$$

For $n'=1,\ldots,2^{j-1}$, we obtain

$$\begin{cases} \int_0^t \psi^{(3)}_{n',0}(\tau)\,d\tau = \frac{1}{2^j}\left(L^{(3)}_{0,0}\psi^{(3)}_{n',0} + L^{(3)}_{0,1}\psi^{(3)}_{n',1} + F^{(3)}_{0,0}\sum_{n=n'+1}^{2^j-1}\psi^{(3)}_{n,0}\right)(x), \\ \int_0^t \psi^{(3)}_{n',1}(\tau)\,d\tau = \frac{1}{2^j}\left(L^{(3)}_{1,0}\psi^{(3)}_{n',0} + L^{(3)}_{1,1}\psi^{(3)}_{n',1} + L^{(3)}_{1,2}\psi^{(3)}_{n',2} + F^{(3)}_{1,0}\sum_{n=n'+1}^{2^{j-1}}\psi^{(3)}_{n,0}\right)(x), \\ \int_0^t \psi^{(3)}_{n',m'}(\tau)\,d\tau = \frac{1}{2^j}\Big(L^{(3)}_{m',0}\psi^{(3)}_{n',0} + L^{(3)}_{m',m'-1}\psi^{(3)}_{n',m'-1} + L^{(3)}_{m',m'}\psi^{(3)}_{n',m'} \\ +L^{(3)}_{m',m'+1}\psi^{(3)}_{n',m'+1} + F^{(3)}_{m',0}\sum_{n=n'+1}^{2^j-1}\psi^{(3)}_{n,0}\Big)(x), \quad \text{for } m'=2,\ldots,M-2 \\ \int_0^t \psi^{(3)}_{n',M-1}(\tau)\,d\tau \approx \frac{1}{2^j}\Big(L^{(3)}_{M-1,0}\psi^{(3)}_{n',0} + L^{(3)}_{M-1,M-2}\psi^{(3)}_{n',M-2} + L^{(3)}_{M-1,M-1}\psi^{(3)}_{n',M-1} \\ +F^{(3)}_{M-1,0}\sum_{n=n'+1}^{2^j-1}\psi^{(3)}_{n,0}\Big)(x), \end{cases}$$

In the same manner, the other matrices can be obtained. ■

The following property of the product of two Chebyshev wavelet functions will be used later:

$$A^T\Psi^{(k)}(x)\left(\Psi^{(k)}\right)^T(x) = \left(\Psi^{(k)}\right)^T(x)\widetilde{A}, \quad \forall k = \overline{1,4}, \tag{10}$$

where, A is a given vector and $\widetilde{A}$ is a $(2^{j-1}M) \times (2^{j-1}M)$ matrix that depends on A [28].

4 Description of the Numerical Methods

In this section, we present the steps that contribute to the solution of the problem (1). We begin by describing an iterative technique to transform our problem to a set of decoupled and linearized differential equations. Then, we use Chebyshev wavelet methods to solve each equation.

The decoupling and quasi-linearization technique consists in giving an initial profile $u_1^{(0)}(x), u_2^{(0)}(x), u_3^{(0)}(x), u_4^{(0)}(x)$ for each solution. The technique can be summarized as

$$\begin{cases} \dfrac{du_1^{(k+1)}}{dx} + b_1u_1^{(k+1)} = f_1\left(x, u_1^{(k)}, u_2^{(k)}, u_3^{(k)}, u_4^{(k)}\right) \\ \dfrac{du_2^{(k+1)}}{dx} + b_2u_2^{(k+1)} = f_2\left(x, u_1^{(k+1)}, u_2^{(k)}, u_3^{(k)}, u_4^{(k)}\right) \\ \dfrac{du_3^{(k+1)}}{dx} + b_3u_3^{(k+1)} = f_3\left(x, u_1^{(k+1)}, u_2^{(k+1)}, u_3^{(k)}, u_4^{(k)}\right) \\ \dfrac{du_4^{(k+1)}}{dx} + b_4u_4^{(k+1)} = f_4\left(x, u_1^{(k+1)}, u_2^{(k+1)}, u_3^{(k+1)}, u_4^{(k)}\right), \end{cases}$$

where, $u_i^{(k+1)}$ and $u_i^{(k)}$ are the approximations of the u_i solution at the current and the precedent iteration, respectively.

At each iteration, the Chebyshev wavelet methods are applied to every linear differential equation. Thereafter, we can calculate the decoupling error by using the following formula

$$E_{DQLT} = \max(E_i), \forall i = \overline{1,4}$$

where,

$$E_i = \left\| u_i^{(k)} - u_i^{(k+1)} \right\|_2.$$

We shall obtain the solution when the error of decoupling is lower than a chosen epsilon.

Now, we consider the following equation

$$a(x)u'(x) + b(x)u(x) = f(x), \quad \text{for } x \in]0,1]], \tag{11}$$

associated with the condition

$$u(0) = u_0, \tag{12}$$

where a, b and f are continuous functions.

Remark 5 *By using the DQLT method, each equation of the reverse osmosis desalination system model presented in (1) can be written as equation (11)*

To solve the problem (11-12), we use the decomposition as (5), indeed,

$$u'(x) = U^T \Psi(x), \tag{13}$$

and

$$\begin{cases} a(x) = A^T \Psi(x) \\ b(x) = B^T \Psi(x) \\ f(x) = F^T \Psi(x). \end{cases} \tag{14}$$

Integrating both sides of (13) over $(0, x)$ and using the theorem 3, we find

$$u(x) = \left(U^T P + u_0 d^T\right) \Psi(x), \tag{15}$$

where, we have used the fact that $1 = d^T \Psi(x)$ as (5).

Substituting (12-13-14) into (11), we get

$$A^T \Psi(x) \Psi^T(x) U + B^T \Psi(x) \Psi^T(x) (U^T P + u_0 d^T)^T = F^T \Psi(x).$$

Thanks to (10), we have

$$\Psi^T(x) \widetilde{A} U + \Psi^T(x) \widetilde{B} (P^T U + u_0 d) = \Psi^T(x) F.$$

Therefore, we obtain the linear algebraic system

$$(\widetilde{A} + \widetilde{B} P^T) U = (F - u_0 \widetilde{B} d). \tag{16}$$

The solution of the problem (11-12) is given by substituting the solution of (16) into (15).

4.1 Test of the methods

In order to demonstrate the efficiency of our approach, we consider the following nonlinear system in $]0, 1]$

$$\begin{cases} u'(x) - u(x) = v(x) + e^x - e^{x+1} \\ v'(x) - v(x) = \frac{u(x)}{v(x)} - xe^{-1}, \end{cases} \tag{17}$$

associated to the boundary conditions

$$\begin{cases} u(0) = 0 \\ v(0) = e. \end{cases} \tag{18}$$

The analytical solution of the problem (17,18) is given as

$$\begin{cases} u_e(x) = xe^x \\ v_e(x) = e^{x+1}. \end{cases}$$

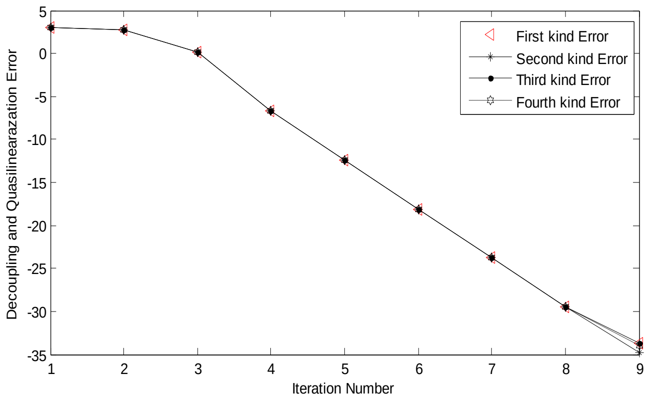

Figure 2: Logarithmic Error induced by DQLT.

The curve in figure 4.1 shows strict decrease of the DQLT error, which explains the convergence about 9 iterations and the stability of the solution produced by four kinds Chebyshev wavelet methods.

Table 2: The Absolute Errors $E(u) = \|u_e - u\|_2$ for $j = 3$.

		k=1	k=2	k=3	k=4
nc=3	E(u)	1.4680e-003	1.7034e-003	1.5026e-003	2.9970e-003
	E(v)	1.0633e-003	1.2485e-003	1.1965e-003	2.0953e-003
nc=10	E(u)	2.2157e-014	4.1452e-015	1.5877e-014	1.4153e-014
	E(v)	3.5988e-014	1.1469e-014	7.6948e-014	1.0943e-013

In Tables 3-4-5-6, the computational point wise errors are listed. The effect of collocation points on the solution profiles is shown. The analysis of the table 2 shows that the absolute error is less than 10^{-13} for 20 collocation points. We consider that the high

Table 3: The point wise errors $|u_e(t_i) - u_i|$ with $j = 2$.

	nc=3				nc=10			
x	k=1	k=2	k=3	k=4	k=2	k=1	k=3	k=4
0	2.3356e-3	4.6588e-3	8.6564e-3	1.1013e-3	1.7764e-15	1.1102e-14	8.8818e-16	4.4409e-16
0.2	1.5941e-3	6.5117e-4	1.4062e-3	2.4150e-5	1.7764e-15	4.4409e-16	9.7700e-15	2.2204e-15
0.4	2.0083e-3	1.1089e-3	1.8921e-3	4.1400e-4	0	8.8818e-16	8.8818e-16	1.7764e-15
0.6	3.7594e-3	7.3048e-4	1.0565e-3	2.3343e-3	8.8818e-15	1.7764e-15	2.6645e-15	2.6645e-15
0.8	1.3783e-3	1.8603e-3	1.2357e-3	2.4510e-3	1.7764e-15	0	5.3291e-15	7.1054e-15
1	4.2002e-3	6.9171e-3	9.6671e-5	1.3257e-2	5.3291e-15	1.8652e-14	6.2172e-15	7.0166e-14

Table 4: The point wise errors $|v_e(t_i) - v_i|$ with $j = 2$.

	nc=3				nc=10			
x	k=1	k=2	k=3	k=4	k=1	k=2	k=3	k=4
0	2.5464e-4	5.0892e-4	9.1768e-4	1.2360e-4	8.8818e-15	2.2204e-15	1.7319e-14	2.2204e-15
0.2	7.2977e-5	2.0899e-4	5.2565e-4	9.0743e-5	1.7764e-15	1.7764e-15	7.9936e-15	3.5527e-15
0.4	2.8931e-4	1.1659e-4	2.5374e-4	1.3021e-5	1.7764e-15	8.8818e-16	8.8818e-16	3.5527e-15
0.6	9.0681e-5	1.1315e-4	1.7749e-5	2.3843e-4	1.7764e-15	0	2.6645e-15	3.5527e-15
0.8	5.4796e-4	2.3388e-4	1.5554e-4	3.0718e-4	5.3291e-15	8.8818e-16	7.1054e-15	2.1316e-14
1	5.4428e-4	1.0107e-3	6.2874e-5	1.9127e-3	1.5099e-14	3.5527e-15	6.2172e-15	7.1942e-14

Table 5: The point wise errors $|u_e(t_i) - u_i|$ with $j = 3$.

	nc=3				nc=10			
x	k=1	k=2	k=3	k=4	k=1	k=2	k=3	k=4
0	2.8324e-3	5.6254e-3	1.0645e-2	1.3064e-3	6.9987e-15	3.7335e-14	7.1958e-14	3.3194e-15
0.2	2.0712e-3	7.3801e-4	1.5933e-3	9.7293e-6	3.8858e-16	1.2212e-15	6.3283e-15	2.7200e-15
0.4	2.3301e-3	1.4537e-3	2.4930e-3	5.5467e-4	2.4425e-15	2.5535e-15	2.2204e-16	6.1062e-15
0.6	5.3887e-3	9.1124e-4	1.9713e-3	3.4280e-3	6.4393e-15	5.1070e-15	6.6613e-15	2.2204e-15
0.8	1.41e-3	2.7284e-3	2.3388e-3	3.0385e-3	4.8850e-15	1.5543e-15	1.3323e-14	4.4409e-16
1	6.2324e-3	9.3088e-3	1.1483e-3	1.8385e-2	7.1054e-15	6.2617e-14	1.5099e-14	1.2479e-13

precision of the solutions for a smaller collocation points is an excellent indicator about the applicability of the proposed methods.

Table 6: The point wise errors $|v_e(t_i) - v_i|$ with $j = 3$.

	nc=3				nc=10			
x	k=1	k=2	k=3	k=4	k=1	k=2	k=3	k=4
0	2.9490e-4	5.8866e-4	1.0715e-3	1.4165e-4	2.0546e-17	3.0358e-17	1.3227e-16	6.5052e-18
0.2	8.4297e-5	2.7289e-4	6.8488e-4	1.0976e-4	1.4433e-15	1.6653e-16	1.9984e-15	3.3307e-16
0.4	3.6442e-4	1.6336e-4	3.4842e-4	8.7304e-6	1.8874e-15	6.6613e-16	1.7764e-15	6.6613e-16
0.6	1.1105e-4	1.7016e-4	1.5771e-4	3.0344e-4	2.4425e-15	2.2204e-16	2.6645e-15	6.6613e-16
0.8	8.1423e-4	3.3248e-4	2.2034e-6	4.9681e-4	5.7732e-15	1.7764e-15	2.8866e-15	1.3323e-15
1	8.0765e-4	1.4315e-3	2.2034e-6	2.7684e-3	5.7732e-15	8.8818e-16	4.4409e-15	7.1054e-15

5 Simulation of Reverse Osmosis Desalination System

In this section, we propose a new numerical solution for the mathematical model described in Section 2.

The proposed approach seems to be very efficient for nonlinear differential systems. Numerical test shows that one important feature of our approach is that it gives a high-quality of solution as well as a stability and a computational speed for a small number of collocation points.

We consider a small-scale reverse osmosis desalination model (1), where the co-current flow pattern is treated as shown in figure 2, The boundary conditions are

$$\begin{aligned} &Q_{sw}(0) = 226.8, \\ &\dot{Q}_{ss}(0) = 2Q_{sw}(0) \\ &Q_{fw}(0) = 0 \\ &\dot{Q}_{fs}(0) = 0. \end{aligned}$$

The membrane specifications and the operating parameters are given in the table 7 obtained from [31, 32].

Table 7: The operating parameters

Parameters	Value
The membrane diameter (D_m)	0.0576 m
Water density (σ_w)	10^3 kg/m^3
Solute permeability coefficient (B_s)	1.12×10^{-4} m/h
Water permeability constant (A_w)	4.2×10^{-13}h/m
Proportionality coefficient (κ)	$1.02\times10^{+12}$ m^2/h^2
Transmembrane pressure (ΔP)	$4.02\times10^{+13}$ kg/m h^2

The flow is carried out continuously tangentially in the membrane. A part of the solution to be treated divides at the level of the membrane in two parts of different concentrations: A part gets through the membrane (permeate) as shown in figure 5-5, a part which does not get through the membrane (retentate) figure 5-5. As it can be seen, the behaviour of curves predicted by the model is very close to these obtained in the literature.

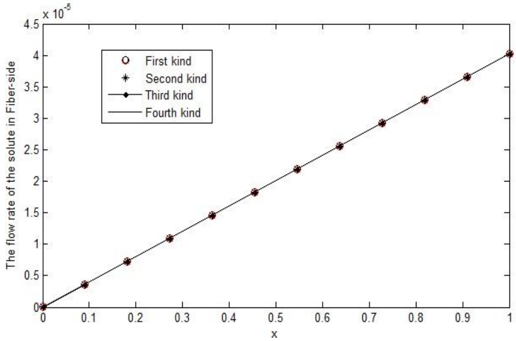

Figure 3: The flow rate of the solute in tube-side.

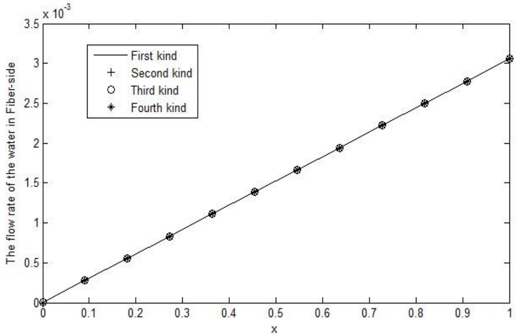

Figure 4: The flow rate of the water in tube-side.

According to the mass conservations laws, the quantity of matter in feed side is the same one which left in permeate and retentate, we get

$$V_1 = Q_{water} - (Q_{permeate\_water} + Q_{retentate\_water}) = 0$$

$$V_2 = Q_{solute} - (Q_{permeate\_solute} + Q_{retentate\_solute}) = 0$$

The examination of the mass conservations laws is pertinante factor for the validation of our simulation. The table 8 shows the quality of the proposed methods for $j = 2$ and

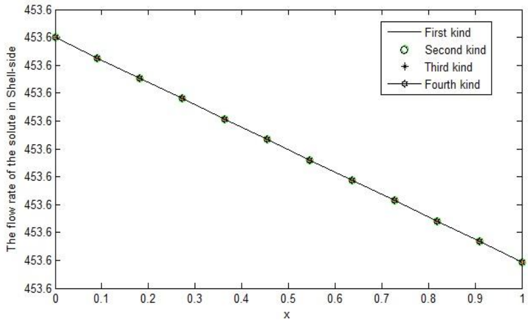

Figure 5: The flow rate of the solute in shell-side.

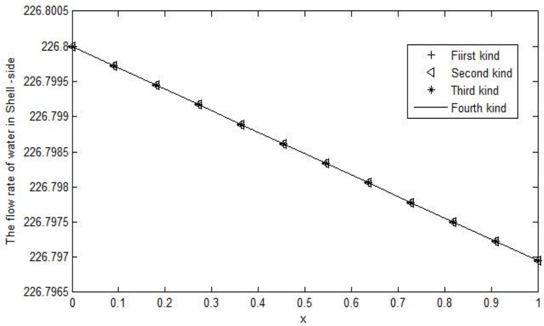

Figure 6: The flow rate of the water in shell-side.

Table 8: Material balance verification.

CWM kth kind	V_1	V_2
k=1	2.0042e-007	7.3896e-013
k=2	6.7535e-009	4.2633e-013
k=3	2.9792e-009	5.6843e-014
k=4	6.5422e-009	2.2737e-013

$nc = 3$, by looking V_1 for the water parameter is of the order of 10^{-9} and V_2 for the solute parameter is less than 10^{-12}.

The obtained result with a few number of collocation points (about 6 points $V_1 = 6.7535e-09$ and $V_2 = 4.2633e-013$ for $k = 2$) was much better than the result obtained with 235 points $V_1 = 3.2909e-008$ and $V_2 = 1.1901e-009$ using orthogonal collocation on the finite element method presented in [2].

6 Conclusion

In this paper, four algorithms for obtaining numerical solutions for small-scale reverse osmosis desalination problem have been analyzed and discussed. The four kinds of Chebyshev wavelets associated with the decoupling and quasi-linearization technique have been employed. This investigation has allowed as to make the following conclusions:

1. As a measure of the high quality and accuracy of approximate solutions, the obtained numerical results are comparing favorably with the analytical solution using a few number of terms of the approximate expansion.

2. The developed algorithms are very effective on natural phenomena.

3. The simulation results of small-scale reverse osmosis desalination model are very close to the experimental data of the literature.

4. The calculation of the difference between the quantity of matter in the feed-side and the permeate-retentate sides shows the quality of the solutions obtained by the proposed methods.

References

[1] A. Abbas, Model predictive control of a reverse osmosis desalination unit, *Desalin.* **194** (2006) 268–280.

[2] B. Absar, O. Belhamiti, Modeling and computer simulation of a reverse osmosis desalination plant-case study of Bousfer plant-Algeria, *Desalin. Water Treat.* **51** (2013) 5942–5953.

[3] B. Absar, S. E. M. L. Kadi, O. Belhamiti, Reverse osmosis modeling with the orthogonal collocation on finite element method, *Desalin. Water Treat.* **21** (2010) 23–32.

[4] W. M. Abd–Elhameed, E. H. Doha, On the coefficients of integrated expansions and integrals of Chebyshev polynomials of third and fourth kinds, *Bull. Malays. Math. Sci. Soc.* **37** (2014) 383–398.

[5] W. M. Abd–Elhameed, E. H. Doha, Y. H. Youssri, New spectral second kind Chebyshev wavelets algorithm for solving linear and nonlinear second–order differential equations involving singular and Bratu type equations, *Abstr. Appl. Anal.* **2013** (2013) 9 pages.

[6] S. A. Avlonitis, K. Kouroumbas, N. Vlachakis, Energy consumption and membrane replacement cost for seawater RO desalination plants, *Desalin.* **157** (2003) 151–158.

[7] E. Babolian, F. Fattahzadeh, Numerical solution of differential equations by using Chebyshev wavelet operational matrix of integration, *Appl. Math. Comput.* **188** (2007) 417–426.

[8] C. Bartels, S. Cioffi, S. Rybar, M. Wilf, E. Koutsakos, Longterm experience with membrane performance at the Larnaca desalination plant, *Desalin.* **221** (2008) 92–100.

[9] O. Belhamiti, A new approach to solve a set of nonlinear split boundary value problems, *Commun. Nonlinear Sci. Numer. Simulat.* **17** (2012) 555–565.

[10] R. Bellman, R. Kalaba, *Quasilinearization and Nonlinear Boundary Value Problems*, Elsevier, New York, 1965.

[11] G. Beylkin, R. Coifman, V. Rokhlin, Fast wavelet transforms and numerical algorithms, *Comm. Pure Appl. Math.* **44** (1991) 141–183.

[12] J. Biazar, H. Ebrahimi, Chebyshev wavelets approach for nonlinear systems of Volterra integral equations, *Comput. Math. Appl.* **63** (2012) 608–616.

[13] J. E. Cadotte, R. S. King, R. J. Majerle, R. J. Petersen, Interfacial synthesis in the preparation of reverse osmosis membranes, *J. Macromol. Sci. A* **15** (1981) 727–755.

[14] S. Coker, P. Sehn, Four years field experience with fouling resistant reverse osmosis membranes, *Desalin.* **132** (2000) 211–215.

[15] I. Daubechies, *Ten Lectures on Wavelets*, SIAM, Philadelphia, 1992.

[16] M. Elimelech, W. A. Phillip, The future of seawater desalination : energy, technology, and the environment, *Science* **333** (2011) 712–717.

[17] J. Sheng, W. S. Jiang, The Haar wavelets operational matrix of integration, *Int. J. Sys. Sci.* **27** (1996) 623–628.

[18] A. Kazemi Nasaba, A. Kiliçmana, E. Babolianb, Z. Pashazadeh Atabakan, Wavelet analysis method for solving linear and nonlinear singular boundary value problems, *Appl. Math. Model.* **37** (2013) 5876–5886.

[19] D. A. Kopriva, *Implementing Spectral Methods for Partial Differential Equations*, Springer, 2009.

[20] R. Kronland–Martinet, J. Morlet, A. Grossmann, Analysis of sound patterns through wavelet tronsforms, *Int. J. Patt. Recogn. Artif. Intell.* **1** (1987) 273–301.

[21] S. Mallat, A theory for multiresolution signal decomposition: the wavelet representation, *IEEE Trans. PAMI* **1** (1989) 674–693.

[22] M. G. Marcovecchio, P. A. Aguirre, N. J. Scenna, Global optimal design of reverse osmosis networks for seawater desalination: modeling and algorithm, *Desalin.* **184** (2005) 259–271.

[23] J. C. Mason, D. C. Handscomb, *Chebyshev Polynomial*, Chapman & Hall, 2002.

[24] O. H. Mohammed, H. A. Ameen, Chebyshev wavelets method for solving partial differential equations of fractional order, *J. Al-Nahrain Univ.* **17** (2014) 185–191.

[25] H. J. Oh, T. M. Hwang, S. Lee, A simplified simulation model of RO systems for seawater desalination, *Desalin.* **238** (2009) 128–139.

[26] C. V. Pao, *Nonlinear Parabolic and Elliptic Equations*, Plenum, New York, 1992.

[27] R. J. Petersen, Composite reverse osmosis and nanofiltration membranes, *J. Membr. Sci.* **83** (1993) 81–150.

[28] M. Razzaghi, S. Yousefi, Legendre wavelets direct method for variational problems, *Math. Comput. Simul.* **53** (2000) 185–192.

[29] T. Rivlin, *The Chebyshev Polynomials*, Wiley, New York, 1974.

[30] J. Shen, T. Tang, L. L. Wan, *Spectral Methods: Algorithms, Analysis and Applications*, Springer, 2011.

[31] C. S. Slater, C. A. Books, Development of a simulation model predicting performance of reverse osmosis batch systems, *Separ. Sci. Technol.* **27** (1992) 1361–1388.

[32] C. S. Slater, J. M. Zielinski, R. G. Wendel, C. G. Uchrin, Modeling of small scale reverse osmosis systems, *Desalin.* **52** (1985) 267–284.

[33] D. Stutson, A. S. Vatsala, Quadratic and semi–quadratic convergence of IVP, *Neural Parallel Sci. Comput.* **3** (1995) 235–248.

[34] A. S. Vatsala, Generalized quasilinearization and reaction diffusion equations, *Nonlin. Times Dig.* **1** (1994) 211–220.

[35] Y. Wang, Q. Fan, The second kind Chebyshev wavelet method for solving fractional differential equations, *Appl. Math. Comput.* **218** (2012) 8592–8601.

[36] X. Wang, Mass transfer and the fluidized bed intensification of reverse osmosis, *Desalin.* **62** (1987) 211–220.

[37] M. Wilf, C. Bartels, Optimization of seawater RO systems design, *Desalin.* **173** (2005) 1–12.

[38] C. Yang, J. Hou, Chebyshev wavelets method for solving Bratu's problem, *Bound. Value Probl.* **2013** (2013) 134–142.

[39] L. Zhu, Y. Wang, Second Chebyshev wavelet operational matrix of integration and its application in the calculus of variations, *Int. J. Compu. Math.* **90** (2013) 2338–2352.